Journal of Organometallic Chemistry, 382 (1990) 445–454
Elsevier Sequoia S.A., Lausanne – Printed in The Netherlands
JOM 20499

Bonding in square-planar $MCl(CX)[P(i\text{-}Pr)_3]_2$ complexes of rhodium and iridium ($X = O$ and CH_2) studied by UV photoelectron spectroscopy and DV-Xα calculations

Carla Cauletti, Felice Grandinetti,

Dipartimento di Chimica, Università "La Sapienza" di Roma (Italy)

Gaetano Granozzi,

Dipartimento di Chimica Inorganica, Metallorganica ed Analitica Università di Padova (Italy)

Maurizio Casarin,

Istituto di Chimica, Università della Basilicata, Potenza (Italy)

Helmut Werner, Justin Wolf, Arthur Höhn and Francesco Javier Garcia Alonso

Institut für Anorganische Chemie, Universität Würzburg (Federal Republic of Germany)

(Received April 11th, 1989)

Abstract

The electronic structure of square-planar rhodium(I) and iridium(I) complexes of general composition *trans*-$MCl(CX)[P(i\text{-}Pr)_3]_2$ ($X = O$ and CH_2) has been investigated by means of gas-phase UV photoelectron spectroscopy (UPS). The results, which are supported by discrete variational DV-Xα calculations, confirm that carbon monoxide and vinylidene act as ligands with very similar properties. The spacing of d orbitals in the iridium complexes seems to be different from that in the rhodium analogues, probably owing to a more significant interaction between the d_{xz} level of iridium and the empty d orbitals of the phosphine ligands.

Introduction

During the rapid development of the chemistry of transition-metal compounds containing metal-to-carbon double bonds [1], transition-metal vinylidene complexes $L_nM{=}C{=}CRR'$ have attracted great interest in the last decade [2]. The parent ligand, $C{=}CH_2$, is not only an isomer of acetylene but also, and perhaps more importantly, isoelectronic species with CO. Since various reports [2,3] seem to indicate that vinylidenes and carbon monoxide have similar donor–acceptor abilities, we thought it of interest to investigate this similarity by means of gas-phase UV photoelectron spectroscopy (UPS). In recent years the use of UPS supported by quantum-mechanical calculations has proved to be very useful in this field [4], and we have also applied it to study the bonding of CO and CS ligands in the half-sandwich type complexes $C_5H_5Co(PMe_3)(CX)$ and $C_5R_5Rh(PMe_3)(CX)$ (X = O, S; R = H, Me) [5].

In the present work, which is part of an extended investigation of the preparation, reactivity, and electronic structure of d^8 transition-metal complexes containing donor–acceptor ligands [6–17], we have studied the gas-phase UV photoelectron spectra of the isoelectronic rhodium compounds, $RhCl(CO)(PR_3)_2$ (**1**) and $RhCl(C{=}CH_2)(PR_3)_2$ (**3**), as well as those of the iridium analogues $IrCl(CO)(PR_3)_2$ (**2**) and $IrCl(C{=}CH_2)(PR_3)_2$ (**4**). These compounds contain two phosphine ligands (namely triisopropylphosphine), a chloride ligand, and a ligand CX (X = O, CH_2), with π-type orbitals capable of interacting with the d orbitals of the central metal atom. It is noteworthy that carbon monoxide is cylindrically symmetric and has two acceptor orbitals, while vinylidene is not symmetric and only has one such orbital. The experimental data (ionization energies, shape and relative intensities of the UPS bands, variation of the intensity ratios between the He(I) and He(II) spectra) are analyzed below in the light of the results of DV-Xα calculations on the model compounds $RhCl(CO)(PMe_3)_2$ and $RhCl(C{=}CH_2)(PMe_3)_2$, respectively, and the results are considered alongside the information from preliminary studies on the reactivity of the square-planar complexes. A brief account of this work has been presented [18].

Experimental

Preparations. The compounds **1** [19], **2** [8], **3** [9,17] and **4** [9,13] were prepared as previously described.

Spectra. The UV photoelectron spectra were recorded on a Perkin Elmer PS 18 spectrometer, modified with a dual He(I)/He(II) lamp, and calibrated with N_2 and self-ionizing helium as internal standards.

Data acquisition temperatures and typical count rates (c.r.) for He(I) spectra were as follows: for compounds **1** $t \simeq 140\,°C$, c.r. $\simeq 10^4$ counts $\cdot\, s^{-1}$; for compound **2** $t \simeq 170\,°C$, c.r. $\simeq 10^4$ counts $\cdot\, s^{-1}$; for compound **3** $t \simeq 120\,°C$, c.r. $\simeq 2 \times 10^3$ counts $\cdot\, s^{-1}$, for compound **4** $t \simeq 120\,°C$, c.r. $\simeq 10^3$ counts $\cdot\, s^{-1}$.

Computational details. SCF Hartree–Fock–Slater (HFS) Discrete Variational DV-Xα calculations [20,21] were carried out on a VAX-8600 computer at the computing center of the University of Padova. A least square fit of the model electronic density to the true density was used to calculate the molecular Coulomb potential [22].

The model charge density was expressed as a superposition of multipolar (MP) densities, where, in addition to atomic radial densities, the expansion basis consists of five localized radial functions multiplied by spherical harmonics with $l = 0, 1, 2$ attached to nuclear sites. Numerical atomic orbitals (AOs) obtained for the neutral atoms were used as basis functions. An extended basis set was used with inclusion of $5d$ AOs for Rh, $3s$ and $3p$ AOs for C and O and $3d$ AOs for Cl and P. Core orbitals ($1s \ldots 4p$ for Rh, $1s$ for C and O, $1s \ldots 2p$ for Cl and P) were frozen and orthogonalized against valence orbitals. For the exchange scaling parameter α, the

Gaspar–Kohn–Sham value [23,24] (2/3) was used. The Mulliken scheme [25] was used to compute atomic orbital populations and overlap populations (OPs). Orbital density plots for some molecular orbitals are also reported and discussed. The experimental ionization energies (IEs) were related to the theoretical values via the Slater's transition state (TS) formalism [26].

Results and discussion

The following complexes were the subject of the present investigation: RhCl(CO)[P(i-Pr)$_3$]$_2$ (**1**), IrCl(CO)[P(i-Pr)$_3$]$_2$ (**2**), RhCl(C=CH$_2$)[P(i-Pr)$_3$]$_2$ (**3**) and IrCl(C=CH$_2$)[P(i-Pr)$_3$]$_2$ (**4**). Taking account of the X-ray structural data for some close analogues of **1**–**4** [9,13,17,27], we assumed that the molecules had a *trans* planar configuration (C_{2v} local symmetry, see the axis system shown in Fig. 1).

The He(I) (21.22 eV) spectra were recorded for **1**–**4** and the He(II) (40.81 eV) spectra whenever this was not ruled out by the low thermal stability of the compounds. UPS literature data for square-planar palladium(II) and platinum(II) complexes containing chlorine and PR$_3$ (R = Me, Et) as ligands [28–30] suggested the presence of a through-space interaction of phosphorus orbitals with orbitals localized on the chlorines and a significant interaction of metal *d* orbitals with Cl orbitals, which is definitely stronger in the platinum compounds. In the discussion below we analyze the effect of the presence of a π-acceptor ligand such as CO or C=CH$_2$ on the composition of the upper MO's and the changes associated with the replacement of rhodium by iridium.

The complexes MCl(CO)[P(i-Pr)$_3$]$_2$ (M = Rh, Ir)

The He(I) and He(II) spectra of these compounds are shown in Fig. 2. In the reported spectral region (up to 10 eV) we expect, on qualitative ground, the presence of nine ionizations from MOs which can be mainly described as (i) four metal based orbitals (d_{y^2}, d_{yz}, d_{xz}, d_{xy}); (ii) two π chlorine orbitals (p_x, p_y); (iii) the two in-phase and out-of-phase linear combinations of the PR$_3\sigma$ levels; and (iv) the $p_z\sigma$ chlorine orbital. The 5σ CO level lies at higher IE. The charge density analysis of the MP-DV-Xα eigenvectors is shown in Table 1 for the nine outermost MOs of **1**, together with the relative TSIEs.

The highest occupied 14 a_1 MO (HOMO) is strongly localized on the Rh atom (75% of d_{y^2}) and includes some minor contribution from the 5σ CO level with a

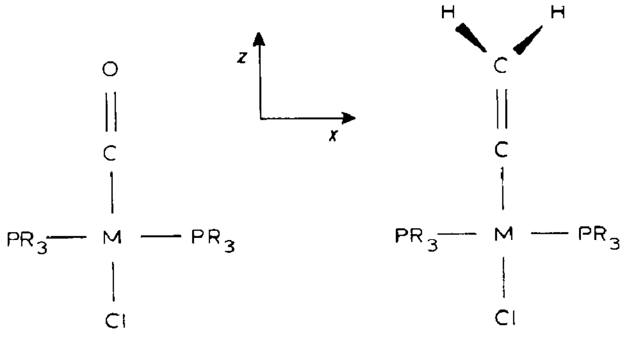

Fig. 1. The coordinate system for molecular orientation.

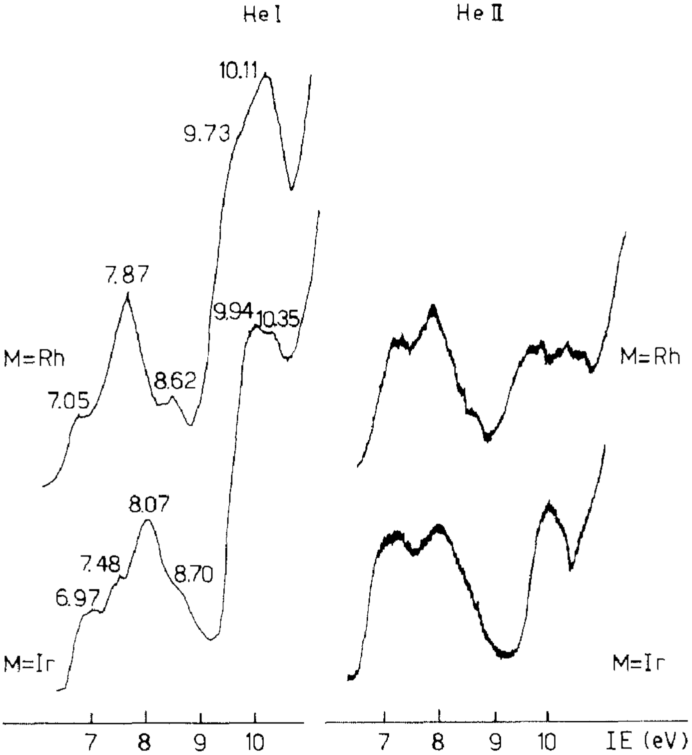

Fig. 2. He(I) and He(II) gas-phase photoelectron spectra of the complexes $MCl(CO)[P(i\text{-}Pr)_3]_2$ (M = Rh, Ir).

small Rh–CO antibonding character. Interestingly, the lowest unoccupied $9b_2$ MO (LUMO) mainly represents the CO $\pi^\star$ level perpendicular to the molecular plane. The computed HOMO/LUMO pattern is in agreement with published electronic

Table 1

Charge density analysis for $RhClCO(PMe_3)_2$ by Mp-SCF-DV-Xα calculations

Symmetry	$-E$ (eV)	TSIE [a] (eV)	Rh			Cl	CO	$2(PMe_3)$	Character [b]
			s	p	d				
$9b_2$(LUMO)	0.69		0	9	17	4	58	12	$\pi^\star(CO)_\perp$
$14a_1$(HOMO)	3.69	6.85	4	0	75	2	11	8	$d_{y^2}+5\sigma(CO)[Rh-Cl]^a$
$11b_1$	4.43	7.65	0	0	18	30	1	51	$d_{xz}+p_\sigma(PR_3)+p_x(Cl)$ $[Rh-Cl]^a$
$6a_2$	4.47	7.69	0	0	92	0	0	8	d_{xy}
$8b_2$	4.55	7.77	0	1	55	28	16	0	$d_{yz}+\pi^\star(CO)_\perp+p_y(Cl)$ $[Rh-Cl]^b$, $[Rh-Cl]^a$
$10b_1$	5.31	8.53	0	1	24	19	10	46	$d_{xz}+p_\sigma(PR_3)$
$7b_2$	6.08	9.30	0	0	24	71	3	2	$d_{yz}+p_y(Cl)[Rh-Cl]^b$
$9b_1$	6.34	9.56	1	0	36	48	4	12	$d_{xz}+\pi^\star(CO)+P_x(Cl)$ $[Rh-Cl]^b$ $[Rh-C]^b$
$13a_1$	6.61	9.83	0	1	1	84	10	4	$p_z(Cl)+5\sigma(CO)$
$12a_1$	7.13	10.35	0	0	29	0	2	69	$d_{y^2}+d_{x^2-z^2}+p_\sigma(PR_3)$ $[Rh-P]^b$

[a] TSIE = transition state IE. [b] Superscript a and b mean antibonding and bonding, respectively.

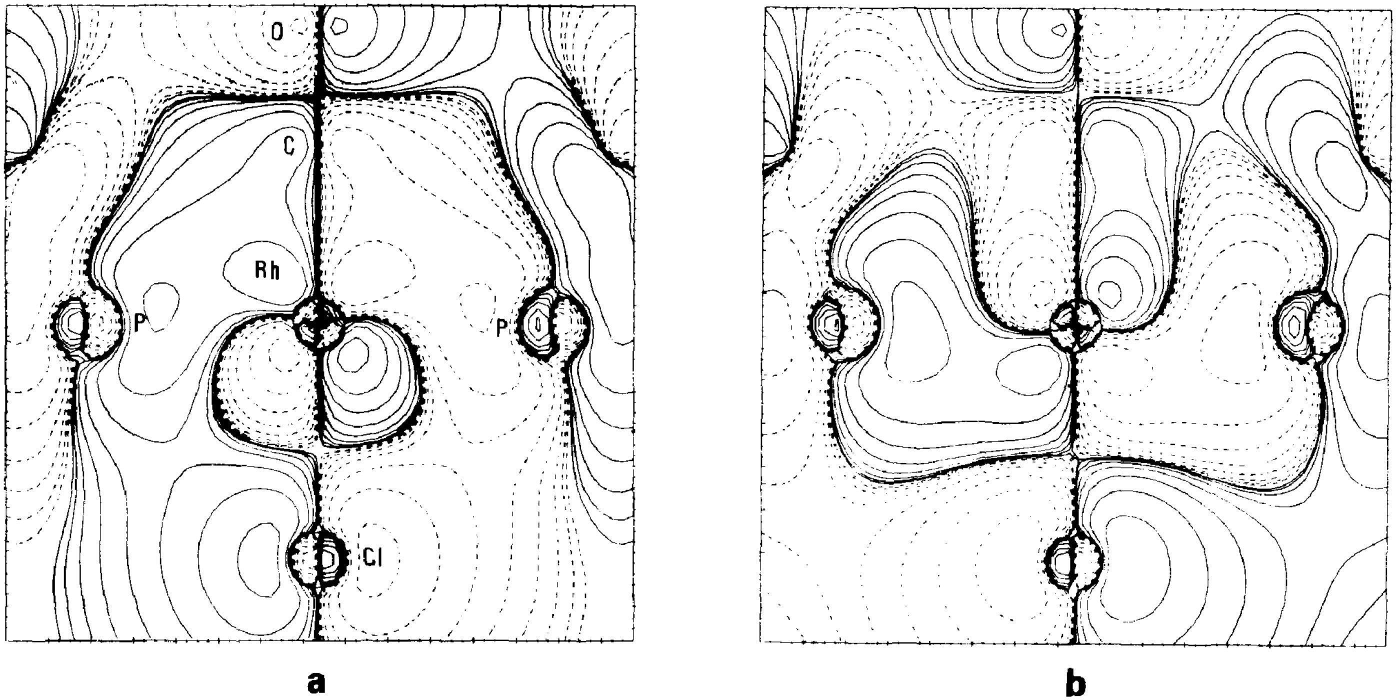

Fig. 3. DV-Xα contour plot of: (a) the $10b_1$ and, (b) the $11b_1$ MO of the complex $RhCl(CO)[P(i\text{-}Pr)_3]_2$. Logarithmic contour levels are ± 1, ± 2, ± 4,... $\times 10^{-3}$ $e^{1/2}/a.u.^{3/2}$.

absorption and MCD spectral data for the analogous $MCl(CO)(PPh_3)_2$ complexes (M = Rh, Ir) [31].

The second highest occupied MO ($11b_1$) is a more delocalized orbital, which can be properly described as an antisymmetric combination of the $PR_3\sigma$ orbitals with d_{xz} of Rh, with a non-negligible contribution of chlorine p_x orbital. The contour plot of this MO in the xz plane is shown in Fig. 3, along with that of the $10b_1$ MO, which has a rather similar composition. The outermost $11b_1$ MO is destabilized with respect to $10b_1$ by a larger Rh–Cl antibonding character. Moreover, a non-negligible in-plane Rh → CO π-donation also contributes to stabilization of the $10b_1$ level. The $6a_2$ MO is a practically pure d_{xy} orbital (92%), while the $8b_2$ orbital is mainly localized (55%) on d_{yz}, with a contribution from $\pi^*(CO)_\perp$ and p_y(Cl). This $8b_2$ MO is antibonding with respect to the Rh–Cl interaction, and is responsible for the back-donation into the $\pi^* \rightarrow (CO)_\perp$ level. Of the following MOs, which are mainly localized on ligand orbitals, $9b_1$ shows a marked metal d contribution (35%) and we suggest that it represents the fourth metal level (d_{xz}) strongly stabilized by in-plane π-bonding interaction with both Cl and CO orbitals.

The bonding emerging from this study is rather different from that in $MCl_2(PR_3)_2$ complexes (M = Pd, Pt; R = Me, Et) [28,30], in which the two highest occupied MOs have a large Cl character with M–Cl antibonding nature. This is, however, excluded in **1** by the comparison between the He(I) and He(II) spectra. In the latter the first band (Fig. 2) is increased in intensity with respect to the subsequent ones, indicating a net predominance of d character in the HOMO. The assignment of the UP spectrum of **1** follows directly from the above analysis, and is supported also by an excellent agreement between theoretical and experimental IE values. The first band, at 7.05 eV, is related to the d_{y^2} $14a_1$ HOMO, the second, peaking at 7.87 eV, arising from the ionization of three MOs, $11b_1$, $6a_2$ and $8b_2$, and the third band (8.62 eV) relates to the $10b_1$ MO. The subsequent intense band, with a maximum at 10.11 and shoulders at 9.73 and 10.43 eV, is associated with several orbitals mainly localized on the ligands. The overall bonding picture emerging from this analysis suggests the presence of a strong Rh → π^*(CO) back-donation, taking place mainly in $8b_2$ ($d_{yz} \rightarrow \pi^*(CO)_\perp$) as indicated also by the calculated overlap populations reported in Table 2.

The He(I) and He(II) spectra of **2** are similar to those of **1**. On the low-energy side of the second band there is, however, a clear shoulder, suggesting a different spacing of the upper MOs. For instance, a greater interaction of d_{xz} of Ir with phosphorus σ orbitals of PR_3 and/or p_x of Cl, destabilizing $11b_1$ MO, is conceivable, and so we suggest that the band at 7.48 eV relates to this MO. However, relativistic effects, such as second order spin-orbit coupling, more important for

Table 2

Overlap populations for the different symmetry representations in $RhCl(CO)(PMe_3)_2$ resulting from Mulliken's population analysis

OP	a_1	a_2	b_1	b_2	Total
Rh–Cl	0.33	0	0.04	0.08	0.45
Rh–C	0.28	0	0.08	0.17	0.53
Rh–P	0.16	0.11	0.13	0.01	0.41
C–O	1.13	0	0.32	0.28	1.73

iridium than for rhodium orbitals, could be responsible for the differing splitting. The assignments of the other features of the spectrum are on the whole the same as for the Rh analogue.

The complexes $MCl(C{=}CH_2)[P(i\text{-}Pr)_3]_2$ (M = Rh, Ir)

The geometry assumed for the theoretical calculation was derived from the X-ray structure of the complex $RhCl(C{=}CHMe)[P(i\text{-}Pr)_3]_2$ [9], which has a *trans*-planar configuration with the hydrogen and the methyl group of the vinylidene ligand lying in a plane perpendicular to the molecular plane. Obviously such a molecular arrangement is important for the bonding scheme. With this geometry the $\pi(C{=}C)$ orbital is composed of p_x-type orbitals (b_1 symmetry) and will interact with d_{xz} of M, while the acceptor orbital (p_y of the α carbon atom) of the vinylidene (b_2 symmetry) will interact with d_{yz}.

The results of the DV-Xα calculations for $RhCl(C{=}CH_2)(PMe_3)_2$ are shown in Table 3. Even though complexes **1** and **3** are isoelectronic, marked differences in the compositions of the computed MOs are found (Tables 1 and 3). This is due to the energy difference between the filled MOs of CO and $C{=}CH_2$, which leads to a better energy matching with metal *d* orbitals in the latter case.

Actually, for compound **3**, the $11b_1$ MO is best described (Fig. 4) as a $Rh(d_{xz})$ $\pi(C{=}C)$ antibonding MO, at variance with the character of the corresponding orbital in **1**. The bonding $Rh(d_{xz})$ $\pi(C{=}C)$ counterpart is represented by the inner $8b_1$ MO. The MO most involved into the $Rh \rightarrow C{=}CH_2$ (p_y) back-bonding is $8b_2$, as in the case of the CO complexes. Comparison between the eigenvalues and the eigenvector compositions of this $8b_2$ MOs in **1** and **3** points to a higher π-acceptor capability for $C{=}CH_2$ than for CO. In this respect, the observed geometrical arrangement of the vinylidene group in the complexes [9] is consistent with the mentioned importance of the M → L out-of-plane back-donation.

Table 3

Charge density analysis for $RhCl(C{=}CH_2)(PMe_3)_2$ by MP-SCF-DV-Xα calculations

Symmetry	$-E$ (eV)	TSIE [a]	Rh			Cl	C′=C″(2)	2(PMe$_3$)	Character [b]
			s	*p*	*d*				
$9b_2$(LUMO)	1.47		0	2	29	5	61	3	$p_y(C')$ vinylidene acceptor orbital
$14a_1$(HOMO)	3.56	6.64	8	0	71	1	11	9	$d_{y^2} + \sigma(C')[Rh{-}C']^a$
$11b_1$	3.97	7.05	0	0	39	20	37	4	$d_{xz} + \pi(C'{=}C'') + p_x(Cl)$ $[Rh{-}Cl]^a$ $[Rh{-}C']^a$
$10b_1$	4.27	7.35	0	0	0	13	13	74	$p_\sigma(PR_3)$
$6a_2$	4.34	7.42	0	0	92	0	0	8	d_{xy}
$8b_2$	4.85	7.93	0	1	24	54	20	1	$d_{yz} + p_y(C') + p_y(Cl)$ $[Rh{-}C']^b$ $[Rh{-}Cl]^a$
$9b_1$	5.68	8.76	0	0	1	56	18	25	$p_x(Cl)$
$13a_1$	6.02	9.10	0	1	1	76	17	5	$p_z(Cl) + \sigma(C')$
$7b_2$	6.04	9.12	0	0	50	39	9	2	$d_{yz} + p_y(Cl) + p_y(C')$ $[Rh{-}Cl']^b$
$8b_1$	6.63	9.71	0	0	37	9	29	25	$d_{xz} + \pi(C'{=}C'')$ $[Rh{-}C']^b$
$12a_1$	6.86	9.94	0	0	27	3	1	69	$d_{y^2} + d_{x^2-z^2} + p_\sigma(PR_3)$ $[Rh{-}P]^b$

[a] TSIE = transition state IE. [b] Superscript a and b mean antibonding and bonding, respectively.

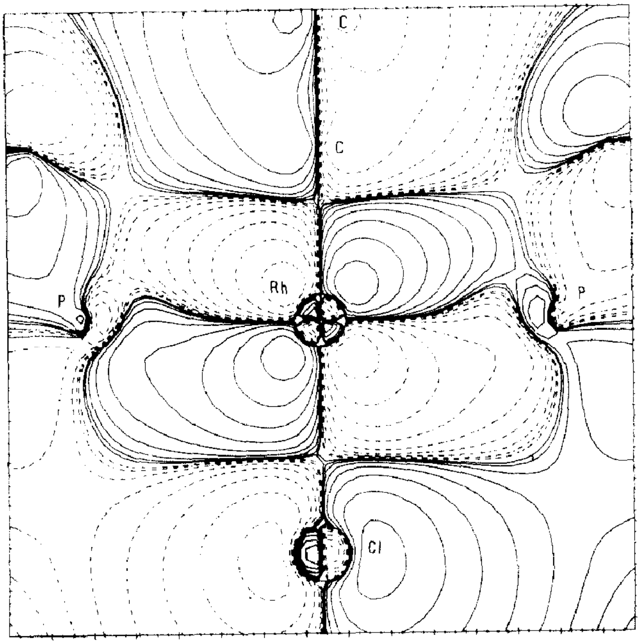

Fig. 4. DV-Xα contour plot of the $11b_1$ MO of the complex $RhCl(C{=}CH_2)[P(i\text{-}Pr)_3]_2$. Logarithmic contour levels are ±1, ±2, $\pm4, \ldots \times 10^{-3}$ $e^{1/2}/a.u.^{3/2}$.

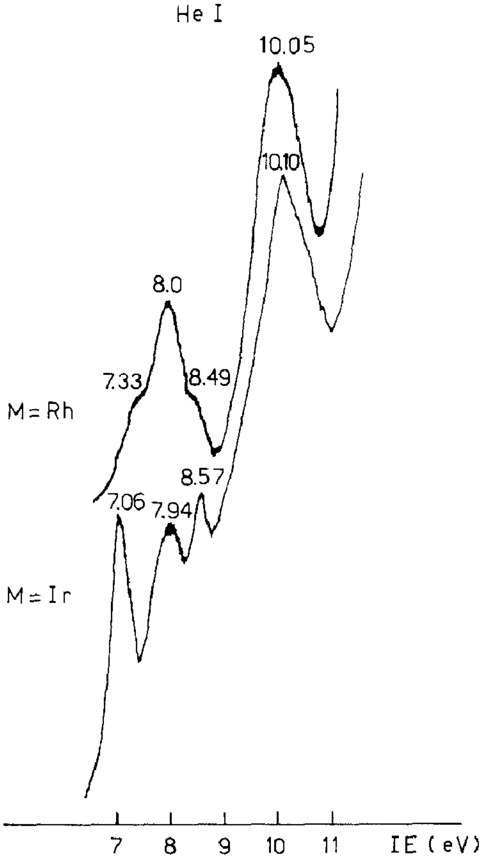

Fig. 5. He(I) gas-phase photoelectron spectra of $MCl(C{=}CH_2)[P(i\text{-}Pr)_3]_2$ (M = Rh, Ir).

The He(I) spectra of **3** and **4** are presented in Fig. 5. The spectrum of **3** shows a shoulder (at 7.33 eV) on the lower IE side of the band centered at 8.0 eV, which is more intense than the corresponding band in the spectrum of **1**. In the light of the calculations, it seems reasonable to assign this shoulder to ionization from both the $14b_1$ and $11b_1$ MOs, bearing in mind also the broad shape of the feature. Consequently, we assign the multi-component band at 8.0 eV to the $10b_1$ and $6a_2$ MOs, and the shoulder at 8.49 eV to the $8b_2$ MO.

The spectrum of **4** is in good agreement with such assignments; again there are stronger interactions between the Ir and the vinylidene ligand. The first band at 7.06 eV is now well resolved, and of comparable intensity with the following one, suggesting that it arises from the ionizations from two orbitals, namely $14a_1$ and $11b_1$. The $11b_1$ MO is destabilized relative to that of the Rh analogue owing to a significantly larger $\text{Ir}(d_{xz})$-π(C=C) repulsion. Similarly, the well resolved band at 8.57 eV is related to the $8b_2$ MO, now shifted toward higher IE because of a more effective $\text{Ir} \rightarrow \text{C=CH}_2(p_y)$ back-donation. Consistently, the band at 7.94 eV is assigned to the $10b_1$ and $6a_2$ MOs.

Conclusion

The results of the UPS measurements and the DV-Xα calculations confirm that in the square-planar complexes $\text{MCl(CO)(PR}_3)_2$ and $\text{MCl(C=CH}_2)(\text{PR}_3)_2$ (M = Rh, Ir) the ligands CO and C=CH_2 show similar bonding properties. The generally accepted view that vinylidene is one of the best π-acceptors known, apparently surpassed only by CS and SO_2 [32], is in full agreement with our data. The charge density analyses for $\text{RhCl(CO)(PR}_3)_2$ and $\text{RhCl(C=CH}_2)(\text{PR}_3)_2$ (see Tables 1 and 3) also reveal why both the carbonyl and the vinylidene complex are good nucleophiles and why they behave as metal bases, reacting not only with acids [10] but also with other electrophilic substrates such as CH_3I [33]. Finally, the stronger metal-vinylidene interactions for iridium than for rhodium support our recent finding that the reaction of $\text{C}_5\text{H}_5\text{Rh(C=CH}_2)\text{P(i-Pr)}_3$ with $\text{IrCl[P(i-Pr)}_3]_2$ does not lead, as in other cases [34], to the formation of a vinylidene-bridged dinuclear complex but gives only compounds **4** [13], i.e., there is a complete transfer of C=CH_2 from rhodium to iridium.

References

1 J.P. Collman, L.S. Hegedus, J.R. Norton and R.G. Finke, Principles and Applications, of Organotransition Metal Chemistry, University Science Books, Mill Valley Calif., 1987; K.H. Dötz, H. Fischer, P. Hofmann, F.R. Kreissl, U. Schubert and K. Weiss, Transition Metal Carbene Complexes, Verlag Chemie, Weinheim, 1983.

2 M.I. Bruce and A.G. Swincer, Adv. Organomet. Chem. 22 (1983) 59 and ref. therein.

3 H. Werner, Angew. Chem., review to be published.

4 For leading references see: (a) C. Furlani and C. Cauletti, Struct. Bonding, 35 (1978) 119; (b) A.H. Cowley, Progr. Inorg. Chem. 26 (1979) 45; (c) J.C. Green, Struct. Bonding, 43 (1981) 37; (d) H. van Dam and A. Oskam, Trans. Metal. Chem., 9 (1985) 125.

5 C. Cauletti, C. Furlani, C. Puliti and H. Werner, J. Organomet. Chem., 289 (1985) 417.

6 J. Wolf, H. Werner, O. Serhadli and M.L. Ziegler, Angew. Chem., 95 (1983) 428; Angew. Chem. Int. Ed. Engl., 22 (1983) 414.

7 H. Werner and A. Höhn, J. Organomet. Chem., 272 (1984) 105.

8 H. Werner and A. Höhn, Z. Naturforsch. B, 39 (1984) 1505.

9 F.J. Garcia Alonso, A. Höhn, J. Wolf, H. Otto and H. Werner, Angew. Chem., 97 (1985) 401; Angew. Chem. Int. Ed. Engl., 24 (1985) 406.
10 A. Höhn and H. Werner, Angew. Chem., 98 (1986) 745; Angew. Chem. Int. Ed. Engl., 25 (1986) 737.
11 H. Werner, J. Wolf, U. Schubert and K. Ackermann, J. Organomet. Chem., 317 (1986) 327.
12 J. Wolf and H. Werner, Organometallics, 6 (1987) 1164.
13 A. Höhn, H. Otto, M. Dziallas and H. Werner, J. Chem. Soc. Chem. Commun., (1987) 852.
14 M. Dziallas and H. Werner, J. Organomet. Chem., 333 (1987) C29.
15 H. Werner, J. Wolf, F.J. Garcia Alonso, M.L. Ziegler and O. Serhadli, J. Organomet. Chem., 336 (1987) 397.
16 H. Werner, T. Dirnberger and M. Schulz, Angew. Chem., 100 (1988) 993; Angew. Chem. Int. Ed. Engl., 27 (1988) 948.
17 H. Werner, F.J. Garcia Alonso, H. Otto and J. Wolf, Z. Naturforsch. B, 43 (1988) 722.
18 C. Cauletti, F. Grandinetti, G. Granozzi, M. Casarin and H. Werner, XXV. International Conference on Coordination Chemistry, Nanjing 1987, Abstr. Papers, Part A1, p. 58.
19 C. Busetto, A. D'Alfonso, F. Maspero, G. Perego and A. Zazetta, J. Chem. Soc. Dalton Trans., (1977) 1828.
20 F.W. Averill and D.E. Ellis, J. Chem. Phys., 59 (1973) 6412.
21 A. Rosen, D.E. Ellis, H. Adachi and F.W. Averill, J. Chem. Phys., 65 (1976) 3629, and ref. therein.
22 B. Delley and D.E. Ellis, J. Chem. Phys., 76 (1982) 1949.
23 R. Gaspar, Acta Phys. Acad. Sci. Hung., 3 (1954) 263.
24 W. Kohn and L.J. Sham, Phys. Rev. A, 140 (1965) 1133.
25 R.S. Mulliken, J. Chem. Phys., 23 (1955) 1833.
26 J.C. Slater, Quantum Theory of Molecules and Solids. The Self-Consistent Fields for Molecules and Solids, Vol. 4, McGraw-Hill, New York, 1974.
27 D.L. Thorn, T.H. Tulip and J.A. Ibers, J. Chem. Soc. Dalton Trans., (1979) 2022.
28 G. Granozzi, G. Zangrande, M. Bonivento and G. Michelon, Inorg. Chim. Acta, 77 (1983) L229.
29 G. Zangrande, G. Granozzi, M. Casarin, J.P. Daudey and D. Minniti, Inorg. Chem., 25 (1986) 2872.
30 J.N. LLouwen, R. Hengelmolen, D.M. Grove, D.J. Stufkens and A. Oskam, J. Chem. Soc. Dalton Trans., (1986) 141.
31 G.L. Geoffroy, H. Isci, J. Litrenti and W.R. Mason, Inorg. Chem., 16 (1977) 1950.
32 A.B. Antonova, N.E. Kolobova, P.V. Petrovsky, B.V. Lokshin and N.S. Obezyuk, J. Organomet. Chem., 137 (1977) 55.
33 A. Höhn, Dissertation Universität Würzburg, 1986.
34 H. Werner, F.J. Garcia Alonso, H. Otto, K. Peters and H.G. von Schnering, Chem. Ber., 121 (1988) 1565.